The influence of chemical structure on isodimorphic behavior of three different copolycarbonates random copolymer series

Idoia Arandia[1], Leire Meabe[1], Nora Aranburu[1], Haritz Sardon[1], David Mecerreyes[1,2], Alejandro J. Müller[1,2*]

[1]*POLYMAT and Polymer Science and Technology Department, Faculty of Chemistry, University of the Basque Country UPV/EHU, Paseo Manuel de Lardizabal 3, 20018, Donostia-San Sebastián, Spain.*

[2]*IKERBASQUE, Basque Foundation for Science, Bilbao, Spain.*

For Table of Contents use only

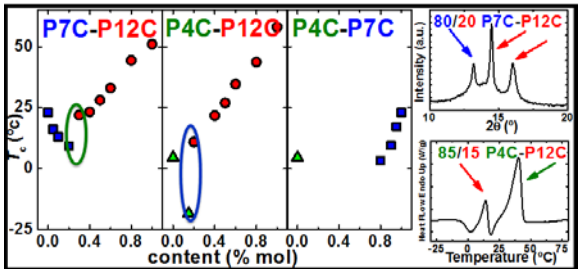

*Corresponding author: alejandrojesus.muller@ehu.es

Abstract

Three series of aliphatic random copolycarbonates, poly(heptane-*co*-dodecane carbonate) P7C-P12C, poly(butane-*co*-dodecane carbonate) P4C-P12C and poly(butane-*co*-heptane carbonate) P4C-P7C, were synthesized by two-step polycondensation process. The organocatalyst 4-(dimethylamino) pyridine (DMAP) was used for the first time to prepare copolycarbonates, as an alternative to metal catalysts, to avoid the toxicity of the remaining catalysts impurities that are difficult to remove after synthesis. Differential scanning calorimeter studies demonstrated the isodimorphic character of the copolycarbonates showing pseudo-eutectic points and the crystallization in a wide composition range. Wide angle X-ray scattering (WAXS) results displayed changes in crystallographic plane spacings possibly due to the isodimorphic behavior of the systems. Two double crystalline copolymers were obtained, i.e., 85/15 P4C-P12C and 80/20 P7C-P12C, as they correspond to pseudo-eutectic compositions. Remarkably, for the 80/20 P7C-P12C copolycarbonate, we found a novel behavior. This copolymer exhibits both coincident crystallization and coincident melting during non-isothermal DSC runs. However, WAXS revealed that the material is double crystalline as it contains crystals from P7C-rich and P12C-rich phases. This is the first example of a double crystalline polymeric material that exhibits a single crystallization and a single melting peak, in spite of being double crystalline. Comparing the results obtained for the 3 series of copolycarbonates, we can conclude that it is easier to incorporate a shorter repeating unit chain segment in a crystal formed by a larger repeating unit chain segment.

Keywords: *copolycarbonates; random copolymers; isodimorphism; crystallization*

Introduction

Aliphatic polycarbonates were first described by Carothers' laboratory at Dupont in the 1930s. Due to their low glass transition temperatures and high susceptibility to hydrolysis, their industrial implementation has not been highly extended. Nevertheless, in this century, studies on aliphatic polycarbonates have shown the importance of this class of materials as versatile biodegradable polymers in the biomedical field, not only due to their high susceptibility to hydrolysis but also because of their biocompatibility and lack of toxicity.[1-5]

Historically, polycarbonates have been synthesized by three different methods: ring-opening polymerization (ROP),[6-9] copolymerization between epoxy and CO_2,[10-12] and by polycondensation between diols and dimethyl or diphenyl carbonate.[13] The polycondensation route is the most appropriate for large scale production and allows tuning the chemical nature of the aliphatic polycarbonates starting from a wide variety of commercially available diols.

The synthesis of polycarbonates by polycondensation is usually catalyzed by metals. Typical examples are: poly(octamethylene carbonate) by TiO_2/SiO_2-poly(vinyl pyrrolidone) based catalyst, TSP-44,[14] copolymers based on poly(butylene carbonate) and poly(hexamethylene carbonate) using the same catalyst,[15] and copolymers of (poly(butylene carbonate) and poly(decamethylene carbonate)) by employing sodium acetylacetonate, NaAcas.[16] Even though these catalysts provide high molar mass aliphatic polycarbonates (100 kg/mol),[17] alternatives are desired in biomedical applications due to the potential toxicity of the remaining catalysts impurities.[13] Thus, the use of organocatalysts is gaining significant interest in the last few years.[13] Among all investigated organocatalysts, 4-(dimethylamino)pyridine (DMAP) has shown so far the best performance in the synthesis of polycarbonates[18,19] and its potential for the preparation of different aliphatic polycarbonates homopolymers.[18,20,21] In spite of the benefits of this catalyst to favor homopolymerization reactions, the use of this catalyst to synthesize copolymers has not yet been exploited.

Random copolymerization has been used widely as a method of combining the properties of two different homopolymers, and in the case of polycarbonates, it is also helpful for limiting

crystallinity degrees and tailoring biodegradation rates. While these aspects have been investigated in the case of polycarbonate copolymers, metal-based catalysts were always used.[15,16,22]

In terms of crystallization, random copolymers can develop isomorphic or isodimorphic behaviors as long as repeating units are not completely excluded from the crystals of the main component. Isomorphism only occurs when repeating units are strictly similar in chemical structure, and therefore, a sigle crystalline phase which contains both repeating units is observed without large variations in their crystal structure over all compositions. In isodimorphic copolymers, depending on composition, two crystal structures which resemble those of the homopolymers are found, while they show a single phase melt. In each phase, repeating units of the minor component are included in the crystal lattice of the major component and vice versa. Upon increasing the concentration of the minor component within the major component rich crystalline phase, the copolymers melting point and crystallinity decrease.[23]

In this work, the synthesis, structure and properties of three series of aliphatic random polycarbonates denoted poly(heptane-*co*-dodecane carbonate) P7C-P12C (odd-even), poly(butane-*co*-dodecane carbonate) P4C-P12C (even-even) and poly(butane-*co*-heptane carbonate) P4C-P7C (odd-even) have been studied. In all cases, different compositions were synthesized using DMAP as organocatalyst in a two-step polycondensation process. The thermal properties, structure, and morphology of all the copolymers were analyzed. A comparison between the three systems was made for the first time in order to identify the differences between copolymerizing even-odd or even-even polycarbonates. For this purpose, the synthesized copolymers have been characterized by Differential Scanning Calorimetry (DSC), Wide Angle X-ray Scattering (WAXS), Polarized Light Optical Microscopy (PLOM) and Small Angle X-ray Scattering (SAXS).

1. Experimental

1.1. Materials

Dry dimethyl carbonate (99+ %) and 4-dimethylaminopyridine (DMAP) (99%) were purchased from Across Organics. 1,4-butanediol (99+ %), 1,7-heptanediol (95%), 1,8-octanediol (99+ %), and 1,12-dodecanediol (98%) were supplied by Across Organics. All diols and DMAP were dried for 5 h before use. Dichloromethane (DCM) (Cerfified AR for Analysis) and methanol (MeOH) (Certified AR for Analysis) were purchased by Fisher Scientific, Tetrahydrofurane (SEC grade) was obtained from Scharlab, toluene (HPLC grace) from Sigma-Aldrich, and deuterated chloroform (99.8%) from Deutero GmbH.

1.2. Synthesis of copolymers: P7C-P12C, P4C-P12C, P4C-P7C

The copolymers were synthesized via melt polycondensation following our previous work.[21] In the first step, dried reagents were introduced in a 50 mL schlenk flask, which was placed in an oil bath at 130 °C, over 4 h. During the second step, the temperature was raised to 180 °C, and high vacuum was applied overnight. Using this methodology, three different polycarbonates families were synthesized, changing the structure of diols and the mol ratio of diols. For all polycarbonates, a molar ratio of DMC:diol:DMAP 2:1:0.01 was used. For instance, P4C-P7C 60:40 mol% was synthesized using the following amounts of reactants: DMC (8 mL, 95 mmol, 2 eq.), diols (1 eq.): 1,4-butanediol (2.57 g, 28.48 mmol, 0.60 eq.), 1,7-heptanediol (2.51 g, 18.99 mmol, 0.4 eq), DMAP (57.9 mg, 0.475 mmol, 0.01 eq.). After the reaction was completed, the polymers were dissolved in dichloromethane and precipitated in cold methanol. ^{1}H NMR was used to confirm the disappearance of the monomers. The final composition of the polymer was determined by ^{1}H NMR ($CDCl_3$, 400 MHz), as an example P4C:P7C, δ= 4.15 (t, OCOOC***H***$_2$, 4H (P4C)), 4.11 (t, OCOOC***H***$_2$, 4H (P7C)), 1.77 (t, $OCOOCH_2C$***H***$_2$, 4H (P4C)), 1.66 (t, $OCOOCH_2C$***H***$_2$, 4H (P7C)), 1.36 (t, $OCOOCH_2CH_2C$***H***$_2C$***H***$_2C$***H***$_2CH_2CH_2OCOO$, 6H (P7C)). The polymerization yield was gravimetrically obtained (yield = 85 %).

1.3. Characterization methods

1.3.1. Magnetic Resonance (NMR)

The ^{1}H and ^{13}C Nuclear Magnetic Resonance (NMR) spectra were registered on a Bruker Avance NEO 500 spectrometer, equipped with a BBOF probe with gradient in Z axis. The 13C spectrum was recorded using a decoupled sequence zgdc from Bruker library at 125.77 Mhz. A time domain of 64k, and a spectral width of 125000 Hz. Interpulse delay 2 s. Acquisition time 2 s. Number of scans 512.

1.3.2. Size exclusion chromatography (SEC)

Size exclusion chromatography (SEC) was employed to determine molar mass distributions. The synthesized materials were dissolved in THF (SEC grade) at a concentration of 5 mg mL^{-1} and then filtered with a 0.45 mm nylon filter. The SEC components were three columns in series (Styragel HR2, HR4, and HR6 with pore sizes ranging from 102 to 106 Å), a precision pump (LC-20A, Shimadzu), an autosampler (Waters 717) and a differential refractometer (Waters 2410). The SEC chromatograms were obtained at 35 °C with a 1 mL min^{-1}flow rate of. Narrow polystyrene standards were employed for calibration, ranging from 595 to $3.95 \cdot 10^{-6}$ g mol^{-1} (5^{th} order universal calibration).

1.3.3. DSC Measurements

The non-isothermal crystallization and melting properties of the homopolymer and copolymer samples were determined with a PerkinElmer 8500 Differential Scanning Calorimetry (DSC). An Intracooler III was used for cooling under ultrapure nitrogen flow and the DSC instrument was calibrated with indium, dodecane and tin standards. The sample mass was kept constant at approximately 5 mg and aluminium pans were used. DSC experiments were carried out in between −40 and +100 °C, and the cooling scans were recorded at 10 °C/min while the heating scans were measured at 20 ºC/min, except for specific experiments performed to determine the glass transitions temperatures. In this last case, the samples were quenched from the melt to −70 °C by employing ballistic cooling (an approximate rate of 250 ºC/min is generated

during ballistic cooling) to try to reduce as much as possible the crystallinity of the samples, then the T_g was determined from the subsequent DSC heating scans performed at 30 ºC/min.

Self-nucleation experiments[24-26] were also performed in two samples, 80/20 P7C-P12C and 85/15 P4C-P12C, to separate the crystallization processes of the two components in the copolymers, as explained below in the text. These experiments were done using scanning rates of 20 °C/min.

1.3.4. Simultaneous SAXS/WAXS Synchrotron measurements

Simultaneous SAXS/WAXS data were obtained at beamline BL11-NCD of the ALBA Synchrotron facility near Barcelona in Spain. For non-isothermal measurements, samples were placed inside capillaries, and employing a Linkam THMS600 hot stage, which was coupled to a liquid nitrogen cooling system, cooling and heating scans were performed at a rate of 20ºC/min, while simultaneous SAXS/WAXS patterns were registered every 0.5 ºC. For the measurements at room temperature, 20 mg of each sample were placed in DSC pans, and SAXS/WAXS patterns were obtained at 25ºC after having cooled them from the melt in the DSC.

For WAXS measurements the wavelength was λ=1.03 Å and a Rayonix LX255-HS detector with an active area of 85 x 255 mm^2 (pixel size 40 μm^2) was employed. The sample to detector distance was 154.69 mm with tilt angle of 29.23˚, and the intensity profile was reported as scattering intensity vs. scattering angle (2θ). In the SAXS configuration, an ADSC Q315r detector, Poway, CA, USA, with a resolution of 3070 × 3070 pixels, pixel size of 102 μm^2 was used. The sample-detector distance was 6495.0 mm with a tilt angle of 0º, and the intensity profiles were reported as scattering intensity versus scattering vector, $q = 4\pi sin\theta\lambda^{-1}$. Silver behenate (SAXS) and chromium (III) oxide (WAXS) were employed to calibrate scattering vectors.

1.3.5 Polarized Light Optical Microscopy (PLOM)

The spherulitic morphology was observed with an Olympus BX51 polarized light optical microscope (PLOM), with a λ plate introduced in between the polarizers at 45°. An Olympus

SC50 digital camera was used to obtain the micrographs, and for a precise temperature control, a Linkam THMS600 hot stage connected to liquid nitrogen was employed. Film samples of copolycarbonates were prepared by casting from chloroform solutions (4 wt %). They were heated 30 °C above their DSC melting peak and kept at this temperature for 3 min to erase thermal history and then they were cooled at 5 ºC/min to -10 ºC where micrographs were obtained.

1.3.6 Dynamic mechanical analysis (DMTA)

For T_g measurements, Dynamic Mechanical Analysis was performed using a TA Instruments DMA Q800 apparatus. Scans were conducted from -100 to 170 ºC at a constant heating rate of 4 ºC/min and a frequency of 1 Hz.

1. Results and discussion

1.1. Synthesis and chemical characterization of copolymers

In this work, the synthesis of 3 different families of random aliphatic polycarbonates was carried out, as shown in Scheme 1. The monomers, 1,4-butanediol, 1,7-heptanediol and 1,12-dodecanediol were co-reacted with dimethyl carbonate using a well-established two-step polycondensation process catalyzed by DMAP where high temperature and vacuum are important requirements to obtain high molar masses.[21] Thus, in the first step, the reaction was maintained at 130 °C during 4 h, whereas for the second step, the temperature was increased until 180 °C and the high vacuum was applied, leaving the reaction running overnight. With this method, a series of different copolymers poly(heptane-*co*-dodecane carbonate) P7C-P12C, poly(butane-co-dodecane carbonate) P4C-P12C and poly(butane-*co*-heptane carbonate) P4C-P7C were synthesized (Scheme 1).

Scheme 1. Polycondensation of diols with dimethyl carbonate leading to random aliphatic polycarbonate copolymers investigated in this work.

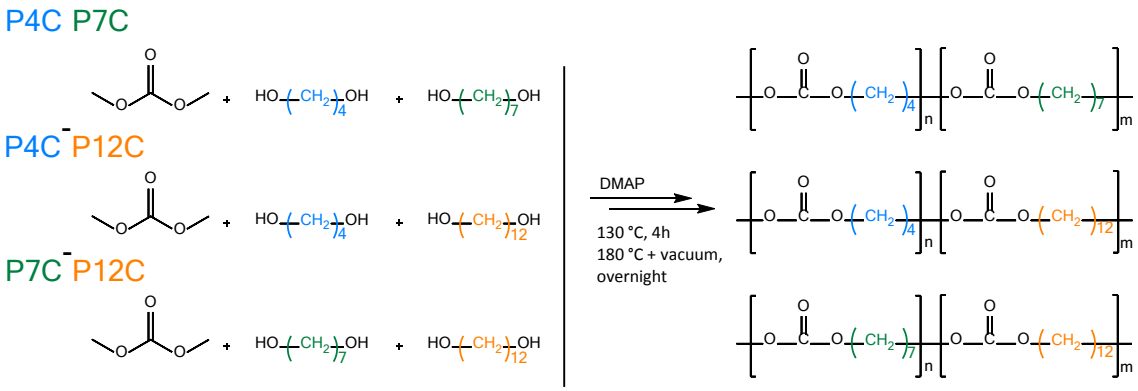

The chemical characterization of the copolymers was carried out by ^{1}H NMR, ^{13}C NMR, and SEC. The molar composition of the copolymers was determined ^{1}H NMR technique. As an illustrative example, the obtained P4C-P7C random copolymer with an initial monomer feed of 60:40 mol% is depicted in Figure 1a. The peak attributed to 3 C$\underline{H}_2$ methylene units in the middle of the repetitive unit corresponding to 1,7-heptanediol, integrates 6 protons. In this way, the value of the rest of the areas will be estimated with respect to that area, and thereby, the mol ratio of the repetitive units can be easily calculated. All the synthesized copolymers were analyzed using similar methodology, and further information is provided in Figure S1 and Figure S2 (see Supplementary Information). The compositions of the 24 copolymers synthesized are given in Table 1. Even if the initial monomer ratio and the final composition in the copolymer are not exactly the same, the final composition was similar to the feed.

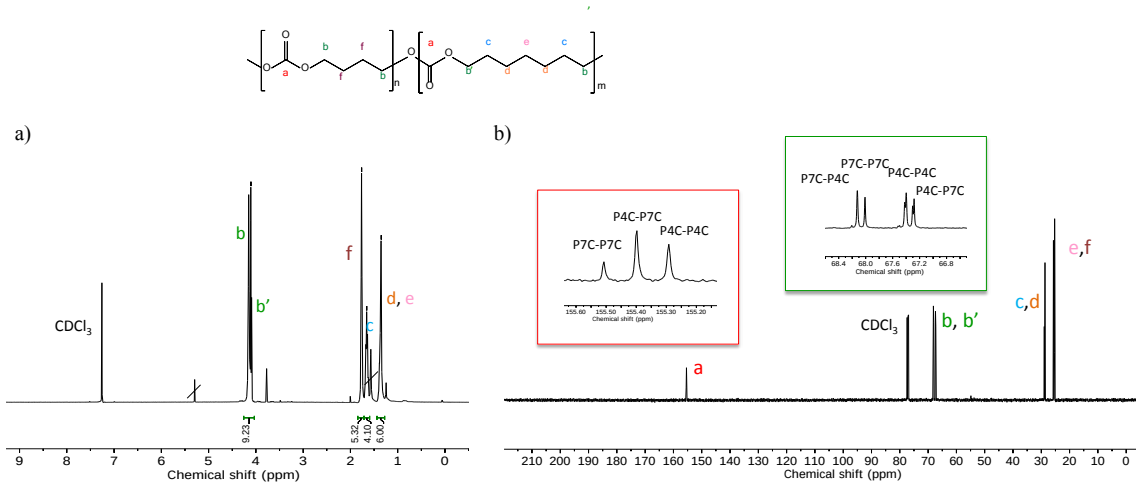

Figure 1. a) ^{1}H NMR of P4C-P7C 60:40 mol% in $CDCl_3$, b) ^{13}C NMR analysis of P4C-P7C 60:40 mol% in $CDCl_3$. The signals of –O<u>C</u>OO- and -OCOO<u>C</u>H_2-, 155.60 – 1555.20 ppm and 68.4 – 66.8 ppm zoomed respectively.

Table 1. Chemical characterization of copolymers: P7C-P12C, P4C-P12C and P4C-P7C.

Initial monomer feed %		**Copolymer composition**		**SEC (PS standard)**		**Randomnes (^{13}C NMR)**
Heptane-diol	**Dodecane-diol**	**P7C**	**P12C**	**M_w**	**Đ**	**R**
95	**05**	95	5	27,000	1.8	0.64
90	**10**	90	10	22,000	1. 7	0.65
80	**20**	82	18	23,000	1.6	0.89
70	**30**	67	33	19,000	1.9	1.13
60	**40**	56	44	32,000	1,6	1.02
50	**50**	43	57	23,000	1,7	0.98
40	**60**	40	60	37,000	1,4	1.15
20	**80**	16	84	31,000	1,6	0.79
Butane-diol	**Dodecane-diol**					
95	**05**	94	6	18,000	1.6	0.77
90	**10**	88	12	15,000	1.3	0.96
85	**15**	82	18	9,500	1.7	1.09
80	**20**	67	33	24,000	1.6	1.07
60	**40**	55	45	16,000	1.5	1.09
50	**50**	43	57	37,000	1.6	1.01
40	**60**	34	66	24,000	1.6	1.06
20	**80**	17	83	24,000	1.5	1.03
Butane-diol	**Heptane-diol**					
95	**05**	92	8	17,000	1.5	0.71
90	**10**	85	15	24,000	1.4	0.72
80	**20**	75	25	35,000	1.6	0.76
60	**40**	66	44	16,000	1.4	1.02
40	**60**	33	67	18,000	1.6	1.04
20	**80**	21	79	9,000	1.6	0.99
10	**90**	10	90	29,000	1.6	0.92
05	**95**	6	94	24,000	1.6	0.62

The comonomer distribution in the copolymer (random, blocky, alternate) is a fundamental factor, which will significantly affect the final properties, such as crystallinity or biodegradation rate. The degree of randomness (R) of the copolymers is defined using equations (1), (2), and (3), and it is determined by ^{13}C NMR analysis.[16] Figure 1b shows the ^{13}C NMR of P4C-P7C 60:40 mol% structure. The signals around 155 and 67 ppm, which are split in three and four peaks, are attributed to the carbonyl and –O**C**H_2 carbon resonance, respectively. A correct assignment of the peaks is necessary to determine the different dyad sequences of the copolymers and consequently, the chemical structure of the copolymer. Additionally, the split of carbonyl resonance is evaluated to determine the microstructure of the copolymer (Figure S3-S5). The degree of the randomness can be obtained applying the following equations:

$$R = \frac{1}{L_{nP4C}} + \frac{1}{L_{nP7C}} \quad (1)$$

$$L_{nP4C} = \frac{f_{P4C-P7C}+2f_{P4C-P4C}}{f_{P4C-P7C}} \quad (2)$$

$$L_{nP7C} = \frac{f_{P4C-P7C}+2f_{P7C-P7C}}{f_{P4C-P7C}} \quad (3)$$

where $f_{P4C\text{-}P4C}$, $f_{P4C\text{-}P47}$, and $f_{P7C\text{-}P7C}$ describe the dyads fraction, whereas L_{nP4C} and L_{nP4C} determine the number-average sequence length of the repetitive units.

The carbonyl resonance is split into three peaks at 155.50, 155.42, and 155.33 ppm, corresponding to the dyads P7C-P7C ($f_{P7C\text{-}P7C}$), P4C-P7C ($f_{P4C\text{-}P7C}$), and P4C-P4C ($f_{P4C\text{-}P4C}$), respectively (Figure 1b). Based on the relative integrated areas (Figure S3-S5) and using 1-3 equations, the microstructure of the copolymers is calculated. Considering that in block copolymers R equals 0, in random copolymers R equals 1, and in alternate copolymers R equals 2, the microstructure of the copolymer is deduced (Table 1). The values are in most cases close to 1, a result that confirms the random nature of the aliphatic copolycarbonates, as expected from the chosen synthetic route. Additionally, the presence of the four dyads could be observed in the methylene –OCH_2 resonances (dyads P7C-P4C, P7C-P7C, P4C,-P4C, P4C-P7, Figure 1b). The randomness character was also confirmed by the integration of the relative areas of the peaks which leads to a similar R value than that calculated with the carbonyl signals.

The molar mass has a direct effect on the thermal properties of the material. Therefore, the molar mass of the material was carefully determined by SEC in THF, using narrow polydispersities PS standards. A similar value for the weight average molecular weight for all copolymers is found, close to 20,000 g/mol (Table 1). The polydispersities obtained by the SEC measurements are common values in polycondensation based synthesis, values between 1.3 and 2.0, (SEC traces can be observed in the **Figure S6**). These similar results facilitate the comparison of the different polycarbonates properties.

1.2. Nonisothermal DSC Measurements

Figure 2 shows the non-isothermal crystallization and melting behavior of P7C-P12C, P4C-P12C, and P4C-P7C co-polycarbonates. Tables 2, 3, and 4 report all transition temperatures and enthalpies.

From a general view of the cooling and heating scans for the three copolymer families, it can be observed that most of the samples exhibit at least one crystallization and melting peak confirming that they crystallized in a wide composition range, even though they are truly random copolymers, as demonstrated by ^{13}C NMR (Figure 1b). Furthermore, their crystallization and melting temperatures strongly depend on composition (Figure 2). The calorimetric results are consistent with isodimorphic behavior.[23,27] Isodimorphism can explain how random copolymers can crystallize in a wide composition range (including 50/50 compositions) forming two crystalline phases that resemble those of the homopolymers. Each rich-phase crystals can incorporate (i.e., crystalline inclusion) some randomly distributed repeating units of the minor comonomer.

Table 2. Calorimetric quantities obtained by DSC for P7C-P12C copolymers.

P7C/P12C	T_g (ºC) DMTA	T_g (ºC) DSC	T_m (ºC)	ΔH_m (J/g)	T_c (ºC)	ΔH_c (J/g)
100/0	-12.3	-50	49.1	53	23.1	55
95/05	-14.1	-50	45.2	39	16.1	45
90/10	-18.4	-47	43.1	43	13.2	48
80/20	**-18.1**	**-45**	**40.4**	**55**	**9.2**	**52**
70/30	-19.2	-43	38.5	70	21.4	61
60/40	-19.4	-44	38.4	60	23.2	59
50/50	-19.7	-42	43.1	75	28.1	59
40/60	-20.1	-39	47.7	64	33.2	62
20/80	-21.9	-34	59.1	75	44.4	72
0/100	-22.1	-35	70.1	64	51.1	99

Table 3. Calorimetric quantities obtained by DSC for P4C-P12C copolymers.

P4C/P12C	T_g (ºC) DMTA	T_g (ºC) DSC	T_m (ºC)	ΔH_m (J/g)	T_c (ºC)	ΔH_c (J/g)	T_{cc} (ºC)	ΔH_{cc} (J/g)
100/0	-15.3	-36	62.1	55	4.5	10	24.9	25
95/05	-13.2	-38	55.2	29			27.1	33
90/10	-14.8	-36	47.6	36			5.3	28
85/15		-39	**40.3/14.1**	**34/2**	**-18.5**	**22**		
80/20		-40	30.8	38	10.9	40		
60/40		-41	40.2	70	21.7	65		
50/50	-16.2	-37	42.7	53	26.9	53		
40/60	-15.3	-36	51.2	54	34.6	54		
20/80	-20.3	-37	59.4	73	43.7	71		
0/100	-22	-35	70.1	64	51.1	99		

Table 4. Calorimetric quantities obtained by DSC for P4C-P7C copolymers.

P4C/P7C	T_g (ºC) DSC	T_m (ºC)	ΔH_m (J/g)	T_c (ºC)	ΔH_c (J/g)	T_{cc} (ºC)	ΔH_{cc} (J/g)
100/0	-36	62.1	55	4.5	10	24.9	25
95/05	-38	50.7	13				
90/10	-39	46.8	8				
80/20	-39	44.1	6				
60/40	-47						
40/60	-50						
20/80	-50	26.2	42	3.2	41		
10/90	-48	41.4	37	9.5	42		
05/95	-50	44.7	39	17.1	50		
0/100	-50	49.1	53	23.1	55		

When the results are analyzed in more detail, it is observed that all P7C-P12C compositions exhibit one crystallization peak (Figure 2a) and one melting peak (Figure 2b) except for neat P7C and the compositions rich in P7C (95/05 and 90/10). These three materials show two

melting peaks in Figure 2b. The origin of these two melting peaks could be due to a partial melting and recrystallization process or to polymorphic behavior. According to the WAXS results presented below, reorganization during the scan is the most likely reason, as no polymorphic behavior was detected.

The P4C-P12C family has a similar behavior as compared with the previous system (Figure 2c and 2d). But in this case, the copolymers where P4C content is larger than 85% did not crystallize during cooling from the melt at 10 ºC/min (Figure 2c), and they undergo cold crystallization during the subsequent melting scan (Figure 2d). This behavior could be explained taking into account that the P4C homopolymer hardly crystallizes at this cooling rate (Figure 2c), and therefore it also shows a large cold crystallization exotherm in the subsequent heating scan (Figure 2d).

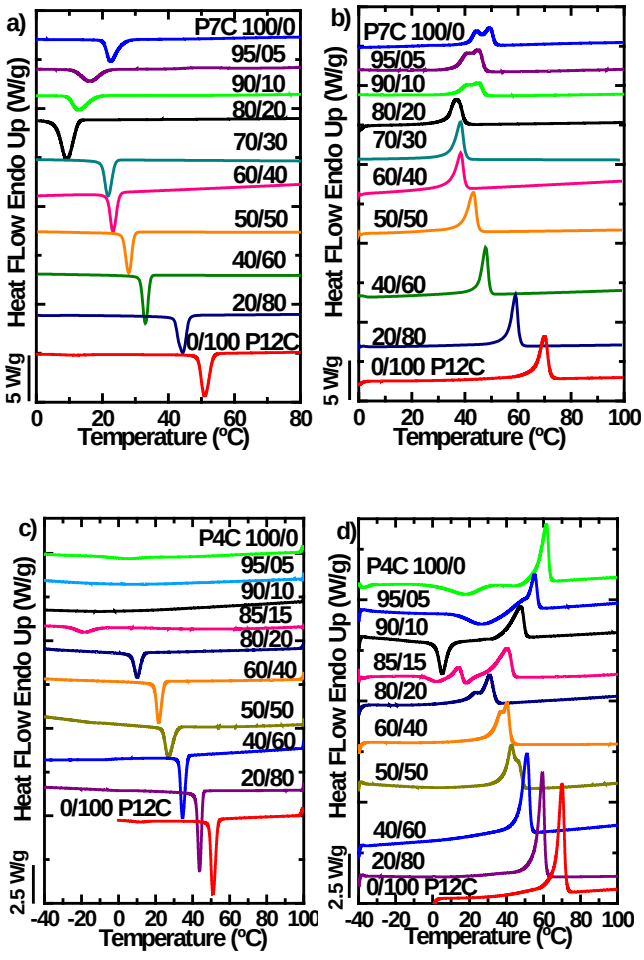

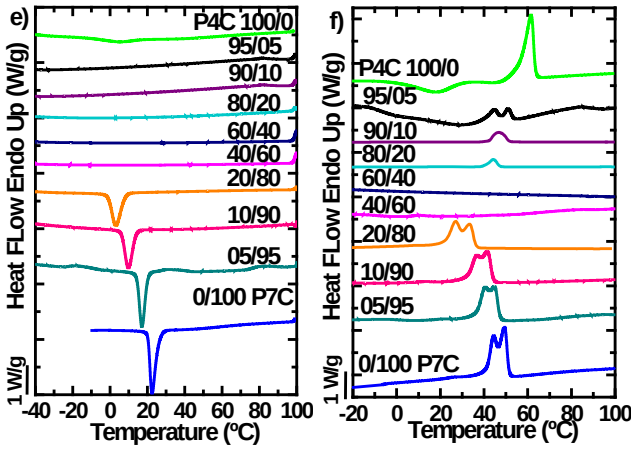

Figure 2. (a), (c) and (e) cooling DSC scans from the melt at 10 ºC/min and (b), (d) and (f) subsequent heating scans at 20ºC/min for the indicated homopolymers and random copolymer samples.

Additionally, 95/05 P4C-P12C and 90/10 P4C-P12C compositions crystallize even less as a result of isodimorphism since, although the incorporation of P12C repeating units is possible (as suggested by WAXS results that will be presented below), most of the minor component repeating units probably act as defects which are excluded from the major component crystalline regions limiting and hindering P4C-rich phase crystallinity.

On the other hand, the 85/15 P4C-P12C random copolymer, which is near the pseudo-eutectic point, can develop a double crystalline structure, and two fully separate melting peaks are obtained during heating (Figure 2d). According to WAXS experiments to be presented below (in Figure 6), these peaks are due to the melting of P12C-rich phase and P4C-rich phase, at low and high temperatures respectively. However, only one sharp crystallization peak, which corresponds to the P12C-rich phase, is observed during the previous cooling scan (Figure 2c).

To further study this double crystalline behavior, self-nucleation experiments[26,28] were performed to this sample and the obtained results plotted in Figure 3. Self-nucleation *Domains* are indicated with different color codes, red for *Domain I*, blue for *Domain II* and green for *Domain III*. Figure 3a shows that when the sample was first cooled from the melt (T_s=100 ºC, in *Domain I*) at a rate of 10ºC/min, only the P12C-rich phase can crystallize (also corroborated by

WAXS in Figure 6a). During subsequent heating, Figure 3b, the P4C-rich phase can undergo cold-crystallization.

However, when the P4C-rich phase is self-nucleated (T_s=46ºC in *Domain II*), Figure 3a, it can crystallize during cooling and a new crystallization exotherm develops at a higher temperature (14 ºC, indicated by an arrow in Figure 3a). Furthermore, at lower self-nucleation temperatures (i.e., 44 and 42 ºC), the P4C-rich phase can crystallize to saturation, while P12C-rich phase`s crystallinity dramatically decreases, evidencing anti-nucleation. As it occurred in previous self-nucleation studies for double crystalline isodimorphic copolymers,[28] this anti-nucleation effect is probably caused by topological confinement produced in the interlamellar domains of P4C. During the subsequent cooling scan, after being self-nucleated, the P4C-rich phase crystallizes first, at higher temperatures, forming spherulites which act as a template for the P12C-rich phase. The P12C-rich phase crystallizes at lower temperatures within the interlamellar spaces of the P4C-rich phase spherulitic template.

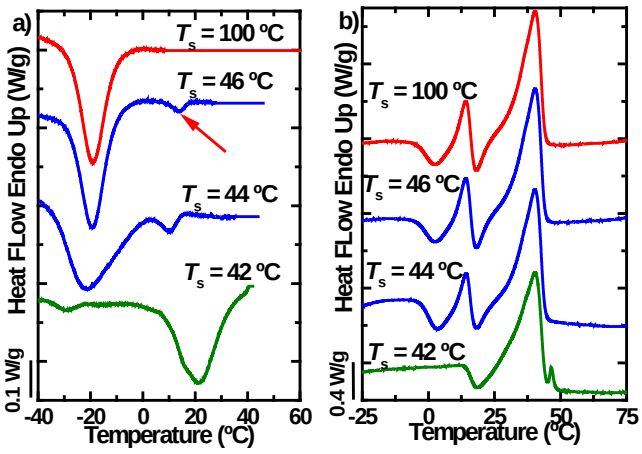

Figure 3. Self-nucleation of 85/15 P4C-P12C: (a) DSC cooling scans from the indicated self-nucleation (T_s) temperatures and (b) subsequent heating scans at 20 °C/min.

Finally, the P4C-P7C copolymers family is the most different system studied here since only compositions higher than 80% of P4C and higher than 80% of P7C were able the crystallize

under the cooling and heating conditions employed. Therefore, not all the compositions show crystallization and melting peaks in the DSC scans (Figures 2e and 2f). Two possibilities could explain these results. Firstly, the inclusion of P4C comonomers within the P7C crystalline phase and vice versa may not be possible, and consequently, the copolymers are unable to crystallize in all the composition range, as it happens when total exclusion occurs.

Total exclusion is the most frequently described case in random copolymers, and it occurs when the chemical structures of the two repeating units are very different from one another, which is not the case of these copolymers. Secondly, despite being isodimorphic copolymers, since the crystallization of both homopolymers is already slow and the exclusion of the minor comonomer units hinders the crystallization, only compositions with more than 80 % of P4C or less than 20 % of P4C can crystallize with the thermal protocol applied. In any case, taking into account the similarities in their chemical structures, it may be possible that crystallization happens if extremely slow cooling is used. Additionally, WAXS results show that small but reproducible crystallographic plane spacings variation occurs as a function of comonomer composition. This evidence, together with the similarities in the chemical structure of the comonomers makes us conclude that this copolycarbonate family is also isodimorphic.

Figures 4a and 4b show plots of peak crystallization and melting temperatures (obtained from Figure 2) for all the systems as a function of composition. All values are a strong function of composition, showing the characteristic pseudo-eutectic behavior of isodimorphic random copolymers. In the case of P7C-P12C and P4C-P12C systems, the eutectic point is found at high P7C and P4C percentages, 80/20 and 85/15, respectively (vertical lines have been drawn at those compositions in Figure 4). In the case of the P4C-P7C system, the pseudo-eutectic point would be at an intermediate composition, between 80 and 20% of P4C if it exists. As in most isodimorphic studies,[23] in these systems the pseudo-eutectic point is found at compositions with higher comonomer content of the homopolymer with a lower melting point.

According to previous studies about isodimorphism,[23] on each side of the pseudo-eutectic point, the copolymer can crystallize in the crystal lattice of one of the components, even if it is not the major component. This result is confirmed by the WAXS results presented below (Figure 5).

In the case of the P4C-P12C system, for compositions with 90% or more P4C content, only P4C-rich crystals are formed, and for compositions with 80% or more P12C content, only P12C-rich crystals are formed. Also, when the composition of the minor component increases, a decrease in the peak melting and crystallization temperature of the mayor component crystals is usually observed due to the frequent interruptions of its linear sequences by the minor comonomer repeating units. Therefore, by choosing carefully the copolymer composition, the copolycarbonates melting point (and therefore their applications) can be tailored from room temperature up to 100 °C.

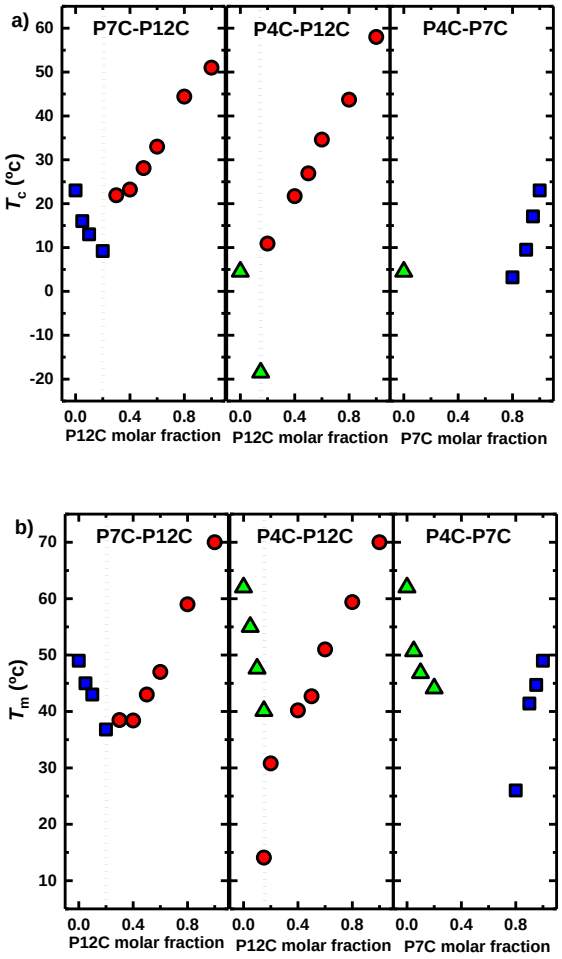

Figure 4. Peak crystallization (a) and melting (b) temperatures as a function of copolymer composition for the indicated systems.

The glass transition temperature (T_g) of all samples was determined using two different experimental techniques. Some of the compositions have a very high crystallinity degree, and this makes difficult the detection of T_g by DSC, therefore for those samples, the T_g was also determined by DMTA. As DMTA applies not only a heating rate but a mechanical stress at a given frequency, the T_g values obtained by DMTA are usually higher than those obtained by DSC, as the equivalent "measurement rate" is much higher in DMTA, and T_g values increases as the heating rate increases. As expected for random copolymers that form a miscible amorphous phase, in these three systems all the copolymers exhibit a single glass transition temperature (T_g) which depends on composition (see Tables 2, 3 and 4) and is located in most cases in between the T_g values of the two parent homopolymers, as expected.

1.3. Wide Angle X-ray Scattering (WAXS)

Figure 5 shows the WAXS patterns for the three synthesized copolymer families obtained at room temperature.

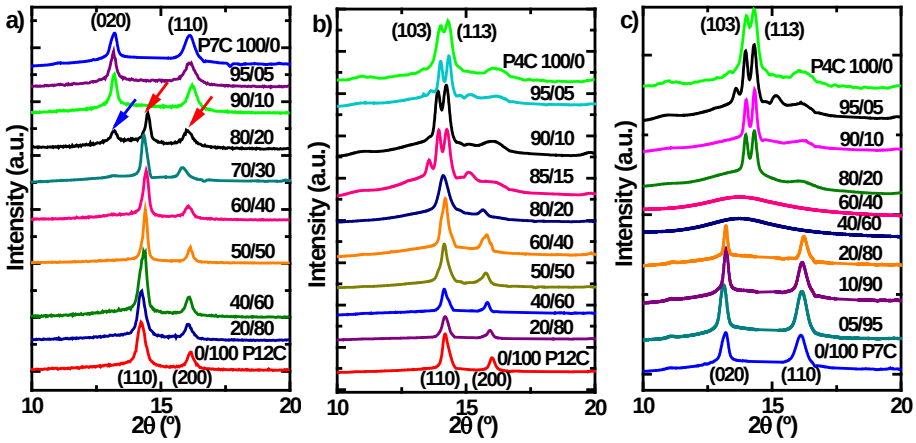

Figure 5. WAXS diffractograms for samples cooled from the melt at 10 °C/min to 25 °C. Measurements were performed at 25 °C. (a) P7C-P12C, (b) P4C-P12C, and (c) P4C-P7C.

The crystalline structures of P7C and P12C have not been reported in the literature as far as we are aware; hence we make tentative assignments to the crystalline reflections observed by WAXS based on data reported for other polymers whose crystalline structure should bear similarities with aliphatic polycarbonates.

The WAXS patterns at 25 °C for P7C-P12C copolymers (Figure 5a) indicate that all samples contain only one type of crystal (either P7C like or P12C like crystal units), except for the 80/20 P7C-P12C composition, which is the only sample showing WAXS reflections corresponding to both homopolymer crystals (see arrows in Figure 5a pointing towards the 80/20 sample diffractogram). The samples with more than 80% P7C, display WAXS patterns that are very similar to that of neat P7C homopolymer. The main crystalline reflections for P7C appear at 13.20º and 16.13º. We have assigned these 2θ values to (020) and (110) planes, as they are consistent with similar crystalline reflections reported for monoclinic unit cells in polytetrahydrofuran.[29] On the other side of the eutectic, those compositions with more than 20% P12C, only display reflections that are consistent with neat P12C homopolymer crystal type. For

P12C, we have assigned the main reflections that appear at 14.18º and 16.00º 2θ values to (110) and (200) planes comparable to those reported for the orthorhombic polyethylene unit cell.[30]

As explained before, although the 80/20 P7C-P12C composition, is close to the pseudo-eutectic point, it only shows one crystallization peak (Figure 2a) and one melting peak (Figure 2b) during the non-isothermal DSC scans. Unexpectedly, in WAXS, it clearly shows reflections that are characteristic of both homopolymers (Figure 5a). Therefore, in this case both crystallization and melting of the two types of crystal phases are coincident in temperature.

For the cooling and heating rates employed (10 ºC/min), the 80/20 P7C-P12C and the 85/15 P4C-P12C compositions (Figure 3) are the only copolymers that can develop double crystalline structures. Different experiments, such as self-nucleation (Figure S7a and S7b in Supporting Information) were performed to the 80/20 P7C-P12C composition, to try to separate the two phases that are present in the sample. WAXS patterns were also obtained every two degrees during cooling and heating scans, as shown in Figures S7c and S7d of the Supporting Information. Nevertheless, as the crystallization of both phases occurs at the same temperature, none of the experiments resulted in the separation of the two phases. Therefore, this copolymer, with composition 80/20 P7C-P12C, exhibits coincident crystallization and melting but it is a double crystalline material, as it contains two distinct crystalline phases (i.e., one P7C-rich crystal phase and one PC12-rich crystal phase). This is the first time we encounter an isodimorphic random copolymer with such peculiar characteristics. Previously, we have only studied isodimorphic copolyesters with coincident crystallization but with clearly separated melting points.[28,31,32]

The other compositions of P7C-P12C copolymers have a typical behavior of isodimorphic random copolymers. The ones with more than 80% P7C only display WAXS patterns characteristic of neat P7C homopolymer and the compositions with more than 20% P12C display reflections that are consistent with a P12C homopolymer type unit cell.

WAXS results at 25 ºC of the P4C-P12C system (Figure 5b) show that all copolymers contain only one type of crystal lattice. The compositions with more than 85% of P4C only display WAXS patterns characteristic of neat P4C homopolymer crystals, whose main reflections appear at 14.04º and 14.33º corresponding to (103) and (113) planes consistent with a monoclinic unit cell.[15,16,33,34] On the other hand, the compositions with more than 15% of P12C display reflections that are consistent with those of a P12C homopolymer which are similar to the orthorhombic polyethylene unit cell, as described above. Even though the DSC results showed two melting peaks for the composition 85/15 P4C-P12C, the WAXS pattern at 25 ºC only shows reflections corresponding to P4C-rich phase, because at this temperature the P12C-rich phase is in the melt state (see Figure 2d).

To study the double crystalline behavior of the 85/15 P4C-P12C copolymer, the sample was first cooled from the melt, down to -20 ºC at 10 ºC/min. Then, WAXS patterns were measured every 2 degrees, while the sample was heated from -20ºC to the melt. Figure 6a shows how reflections of both phases are seen depending on the temperature. Furthermore, from the WAXS patterns obtained during the heating scan, the intensity values of the reflections of both phases (denoted with the numbers 1, 2 and 3, as indicated in the WAXS diffractogram of Figure 6b) were measured and plotted as a function of temperature in Figure 6b.

When the sample was cooled from the melt at a rate of 10ºC/min, only the P12C-rich phase could crystallize, and therefore in Figure 6a at -20 ºC, only the two peaks corresponding to the P12C WAXS reflections (peaks 2 and 3) are observed. As the temperature increases the intensity of these two peaks decreases until they disappear at 10 ºC (Figure 6b). The same behavior occurs in the DSC results, where the first melting peak ends at this temperature (Figure 2d). At 6 ºC, a new peak appears (peak 1), whose intensity increases, displaying a maximum at 24 ºC (Figure 6b). This new reflection belongs to the P4C-rich crystalline phase that cold crystallizes during heating, like neat P4C. Hence, from 5 ºC to 10 ºC, both crystalline phases co-exist.

It is worth noting that the WAXS results at 25ºC of the 85/15 P4C-P12C sample show two new reflections (see Figure 5b), to the left and to the right of the characteristic double-peak of the P4C-rich phase (identified on the WAXS spectrum for P4C as (103) and (113) reflections), which are not consistent with any reflection of P4C and P12C homopolymers. These new peaks also appear in some of the copolymers like 95/05 P4C-P12C and even in 95/05 P4C-P7C. A more detailed crystallographic study would be needed to ascertain the origin of these new reflections in these copolycarbonates, which could correspond to a new crystallographic phase.

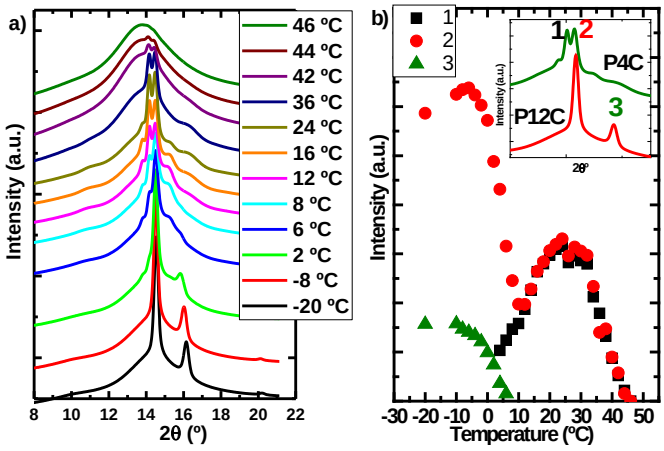

Figure 6. (a) 85/15 P4C-P12C WAXS patterns at the indicated temperatures, (b) Intensity values obtained from Figure **6**a as a function of temperature.

In the case of P4C-P7C copolymers, it was not possible to obtain WAXS patterns for the intermediate compositions at 25 ºC, such as 60/40 and 40/60 P4C-P7C (Figure 5c), as they are molten at room temperature. However, they were expected not to show any reflections since DSC results did not detect any crystallization or melting peaks for these copolymers (Figure 2f). Only compositions with more than 80 % of P4C could crystallize, displaying P4C like WAXS patterns, and in the other side, compositions with more than 80 % of P7C could crystallize, developing, in this case, WAXS patterns characteristic of the P7C crystalline phase.

The crystallinity degree for all systems (Figure 7) was calculated from the WAXS diffraction patterns obtained at room temperature, after cooling all samples from the melt at a rate

of 10 ºC/min. In this case, results also display a pseudo-eutectic behavior, when they are plotted as a function of composition, as a consequence of comonomer exclusion during crystallization, which predominates over comonomer inclusion.

Figure 7 reveals an interesting trend on how crystallinity decreases upon comonomer addition. If the copolymers were isomorphic and all chains could co-crystallize (i.e., 100% inclusion in the crystal lattice of both types of chains), the crystallinity would follow a linear trend with composition. In the case of isodimorphic random copolymers, there is a competition between inclusion and exclusion of the two comonomers inside the crystal lattice. Exclusion causes interruptions of linear crystallizable sequence lengths, and this is manifested in decreases in T_c, $T_{m,}$ and crystallinity.

Please note how in Figure 7, for the PC7-PC12 copolymers, the addition of PC7 to PC12 (right-hand side of the pseudo-eutectic point), only causes very small decreases in crystallinity. However, on the left-hand side of the pseudo-eutectic point, incorporating PC12 to a PC7 chain causes a much larger decrease in crystallinity. These results indicate that it is easier to include PC7 comonomeric units into PC12 crystals than vice-versa. Similar behavior is displayed by the PC4-PC12 family. These results may be rationalized by the differences in repeating unit chain lengths within the crystal lattice. It is probably easier to incorporate a shorter repeating unit chain segment in a crystal formed by a larger repeating unit chain segment.

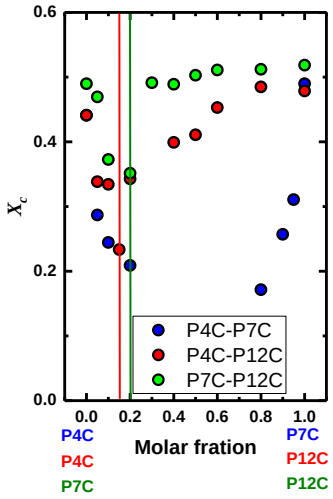

Figure 7. Crystallinity degree determined by WAXS as a function of composition for the indicated copolymers.

Due to the difficulties to crystallize, P4C-P7C copolymers show the lowest crystallinity values when the results of the three systems are compared. For example, the crystallization of copolymers rich in P7C is much more hindered when they are copolymerized with P4C (with adding a 0.5 molar fraction of P4C its crystallinity degree decreases 40 %) than when they are copolymerized with P12C (with 0.5 molar fraction addition of P12C, crystallinity only decreases 5%). These results are also consistent with those obtained by other experimental techniques, like DSC and SAXS, where it is corroborated that the intermediate compositions of P4C-P7C are not even able to crystallize.

In isodimorphic cases, X-ray diffraction results are also used to detect the partial inclusion of the minor comonomer into the crystalline structure of the major component by checking the differences in *d* spacing between crystallographic planes. When the crystals of one of the phases host repeating units from the minor comonomer, different situations have been found in the literature.[35] Upon inclusion of a comonomer unit, the crystalline unit cell of the rich phase can increase in size to accommodate the extra bulkier co-unit, reduce in size in certain directions when the minor comonomer has a lower volume, or in some cases remains unchanged.

When analyzing *d* spacings values of all systems (Figure 8) as a function of composition, the three situations explained above are found. On the one hand, in the three systems, the unit cell

dimensions tend to increase for compositions rich in the comonomer with a lower number of CH_2 units (i.e., P4C in P4C-P7C; P4C in P4C-P12C and P7C in P7C-P12C system), when longer chain comonomer units are included in the crystals. This enlargement in *d* values indicates that P4C and P7C crystal unit cells have to increase their volume to accommodate the extra bulkier repeating units.

Inclusion of comonomer units with lower number of CH_2 in the unit cell of crystals formed by comonomers with a higher number of CH_2 units, leads to different situations, for instance:

(a) in the case of P7C-rich compositions of the P4C-P7C system, *d* values reduce with P4C content as a result of a lower volume occupied by P4C units,

(b) for P12C-rich compositions of the P4C-P12C system, *d* values increase with P4C content. This is an unexpected trend, that is probably a result of including multiple PC4 comonomer units together with PC12 in the crystal, as they are even/even comonomers.

(c) for compositions rich in P12C of the P7C-P12C system, *d* values remain constant (200) or decrease slightly (110), as in this case the comonomers exhibit the lowest difference in size of the 3 series and PC7 possibly fits well the PC12 unit cell with a slight unit cell contraction.[35,36]

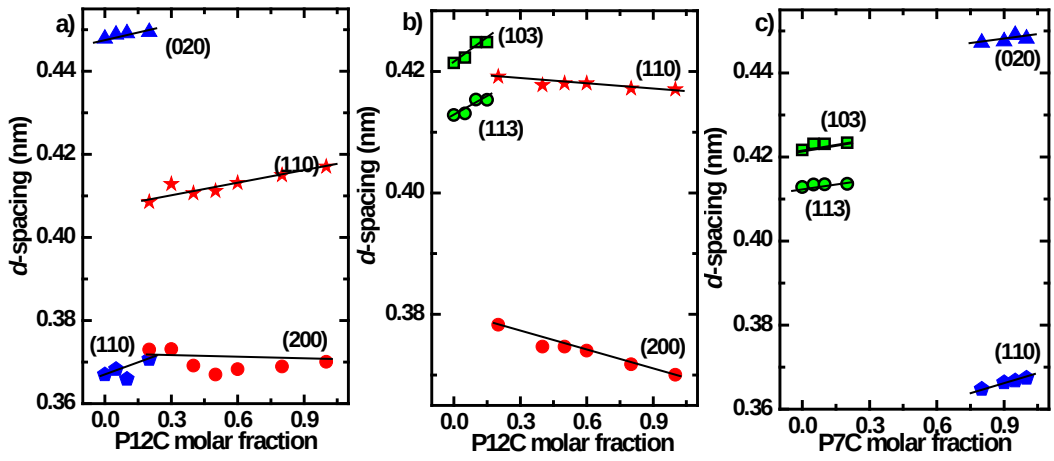

Figure 8. Diffraction spacings (*d*) of the indicated planes as a function of copolymer composition for the three systems. (a) P7C-P12C, (b) P4C-P12C and (c) P4C-P7C.

1.4. Small Angle X-ray Scattering (SAXS)

SAXS results at 25 °C, after having cooled the samples from the melt (at 10 ºC/min) are shown in Figures 9a, 9b and 9c, where the intensity is plotted versus the scattering vector *q*.

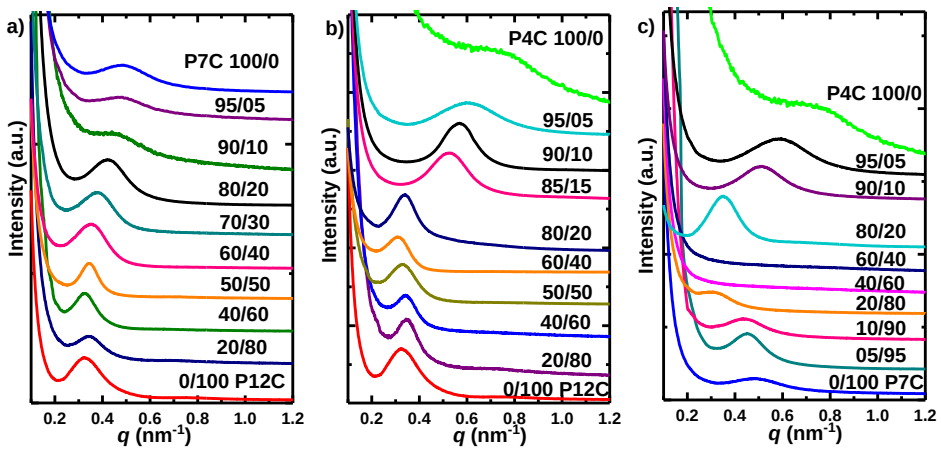

Figure 9. SAXS patterns for the indicated homopolymers and copolymers of the three copolycarbonate systems synthesized in this work. Measurements performed at 25 °C. (a) P7C-P12C, (b) P4C-P12C, and (c) P4C-P7C.

For the three systems, all samples which were found to be semi-crystalline at these conditions exhibit one intense maximum caused by the scattering of lamellar stacks. These results also show that for the intermediate 80/20 P7C-P12C composition, where the two phases could potentially crystallize at 25ºC, two long periods are not observed, as it happened in other isodimorphic copolymer systems.[28] In this case, both homopolymers exhibit similar long periods and in the copolymer, even if two crystalline phases form, their long periods overlap. In the case of P4C-P12C and P7C-P12C, the SAXS peak maxima of the copolymers are located at q values that are in between those corresponding to the peaks of both homopolymers. On the other hand, different results are found for the P4C-P7C system, where the addition of both comonomers increases the value of long period in comparison with both homopolymers.

Using equation (4), long period values were obtained for all crystalline samples and plotted in Figure 10a in which a vertical line has been drawn where the pseudo-eutectic point of each system is located.

$$d^* = (2\pi)/q_{max} \quad (4)$$

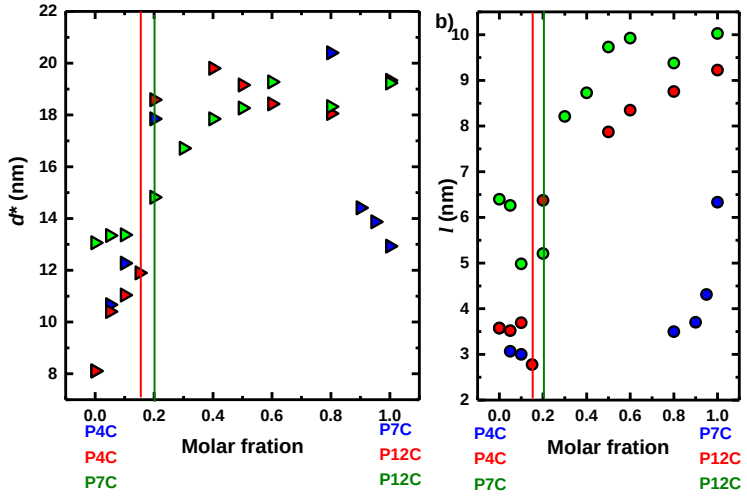

Figure 10. (a) Long periods (d^*) measured by SAXS as a function of copolymer composition. (b) The calculated lamellar thickness for the d^* values shown in (a).

As explained above, the two systems, P4C-P12C and P7C-P12C, have similar behavior concerning the long period. For copolymers rich in P4C and P7C units, the long period increases with P12C and remains almost constant for compositions rich in P12C. On the other hand, in the case of P4C-P7C system, the addition of both comonomers increases the value of long period in comparison with each homopolymer. This increase in long period can correlate with changes in lamellar thickness and/or interlamellar regions. As it was observed in Figure 7, especially in this system, the crystallinity degree of copolymers largely decreases when compared with both homopolymers. A higher amount of amorphous phase could be contributing to an increase in the long period values since this does not occur for the P12C-rich compositions in the other systems where crystallinity degree remains almost constant.

Using equation (5), lamellar thickness (l) values have also been calculated and plotted in Figure 10b.

$$l = d^* x_v \quad (5)$$

x_v is the crystalline volume fraction, which we have approximated to the mass fraction of crystals (x_m), determined from WAXS patterns, because the density of the different copolymers has not been measured as a function of temperature.

The calculated values exhibit, for the three systems, a decreasing trend in l with the addition of minor comomoner content, as a consequence of the incorporation of those comonomers into the chains that limit the length of crystallizable sequences. As it has been seen in previous results, the P4C-P7C system is the most affected in terms of crystallization, and this is reflected with the largest reduction in lamellar thickness. It is worth noticing that the behavior of the lamellar thickness as a function of composition (Figure 10b) exhibits a minimum value close to the pseudo-eutectic point, correlating qualitatively with Figures 4 and 7, especially for P4C-P12C and P7C-P12C copolycarbonates. Such a good correlation indicates the importance of the comonomeric inclusion/exclusion balance that occurs during crystallization in isodimorphic random copolymers.

1.5. Polarized Light Optical Microscopy (PLOM)

In order to study the effect of copolymer composition on the spherulitic morphologies, PLOM micrographs of some of the compositions were taken at -10ºC after cooling the samples from the melt at a rate of 5 °C/min. At this temperature spherulites were already impinged on one another. As seen in Figure 11, the three homopolymers show a relatively high nucleation density, which makes very difficult any study on spherulitic growth or nucleation kinetics. Also, as predicted by the results described above, copolymerization affects the structure of the samples, and in this case, the composition changes the morphology as the copolymers micrographs show an increase in nucleation density (in comparison with homopolymers) and consequently a reduction in spherulitic size.

On the other hand, the study of morphology has also been used to analyze the double crystallization shown by some of the intermediate isodimorphic copolymers. Safari et al.[37] and

Arandia et al.[28] observed by PLOM double crystalline superstructures for PBS-*ran*-PCL and PBS-*ran*-PBAz copolyesters. They reported a higher birefringence when PCL-rich or PBAz-rich phases crystallized inside the spherulitic semi-crystalline template previously formed (i.e., at higher temperatures during cooling from the melt) by PBS-rich phase spherulites. In this case, the high nuclei density also hinders the analysis of the double crystallinity showed by 80/20 P7C-P12C and 85/15 P4C-P12C compositions, where similar results to those obtained in previous works would be expected.

In semi-crystalline polymers, mechanical properties are usually related to the spherulitic size. For that reason, copolymerization has often been used as a way to tailor mechanical performance by modifying the composition.[38,39]

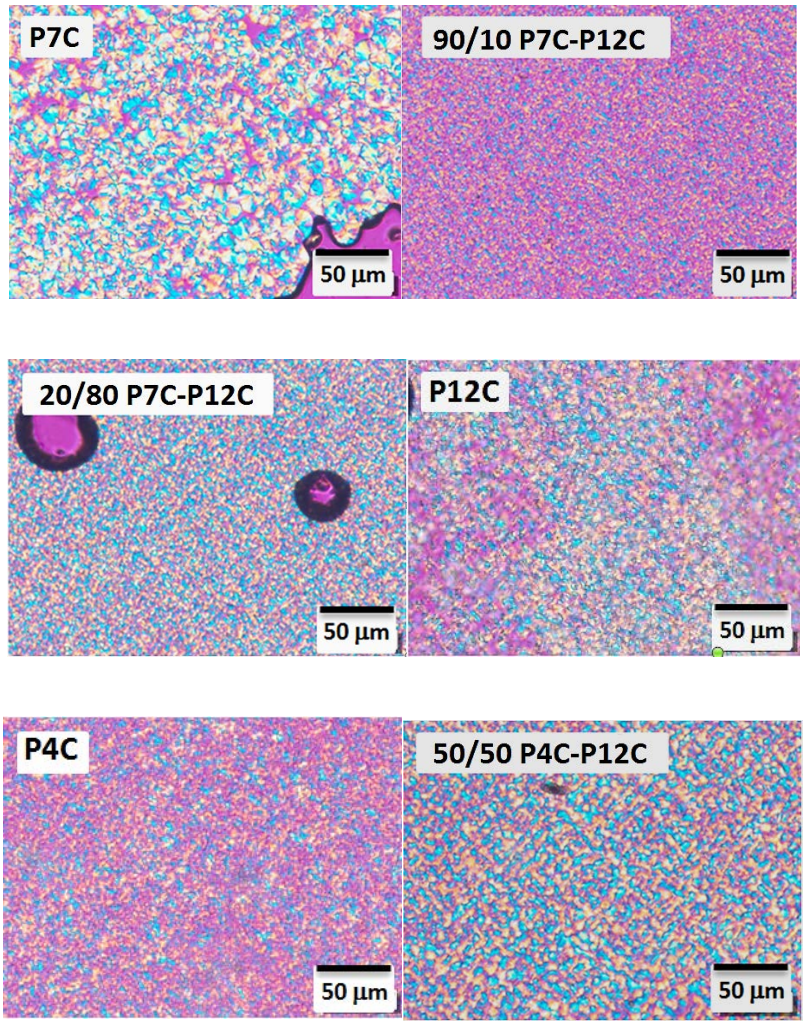

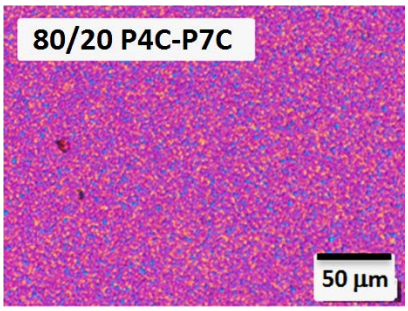

Figure 11. Polarized light optical micrographs for the indicated polycarbonates and copolycarbonates copolymers taken at -10 ºC.

2. CONCLUSIONS

Three series of random copolyesters were successfully synthesized by using a DMAP organocatalyst: P7C-P12C, P4C-P12C, and P4C-P7C, in a wide composition range. After analyzing the molar masses by SEC and the randomness of the materials through ^{13}C NMR, results show that all copolymers have a similar molecular weight (20 kg mol^{-1}) and are truly random. The isodimorphic character of the copolymers was demonstrated by DSC (presence of pseudo-eutectic points, crystallization of most compositions except for one of the systems) and by WAXS (changes in crystallographic plane spacings). For 80/20 P7C-P12C and 85/15 P4C-P12C (i.e., compositions at the pseudo-eutectic points), the copolycarbonates can develop double crystallinity. In the case of 85/15 P4C-P12C, the material exhibit coincident crystallization of both phases (which can be separated by self-nucleation) and separate melting. Such a behavior has been already reported in isodimorphic copolyesters and also in double crystalline diblock copolyesters, but never before in copolycarbonates. Remarkably, for the 80/20 P7C-P12C copolycarbonate, we found a novel behavior. This copolymer exhibits both coincident crystallization and coincident melting during non-isothermal DSC runs. However, WAXS revealed that the material is double crystalline as it contains crystals from P7C-rich and P12C-rich phases. This is the first example of a double crystalline polymeric material that exhibits one crystallization and one melting peak, in spite of being double crystalline.

WAXS results revealed small reproducible variations in the crystalline unit cell of the dominant crystalline phase due to the inclusion of minor comonomer units. Moreover, these unit cell differences showed that the incorporation of shorter comonomer units into larger comonomer unit crystals is more probable, as well as when both comonomers are even (i.e., even/even copolycarbonates).

Supporting Information

^{1}H NMR characterization of P7C-P12C 70/30 and P4C-P12C 50/50 copolymers, ^{13}C NMR characterization of P7C-P12C, P4C-P12C and P4C-P7C copolymer systems with different mole ratios. Self-nucleation DSC and WAXS experiments of P4C-P12C 85/15 copolymer sample.

Acknowledgements

We acknowledge funding from the European Union´s Horizon 2020 research and innovation programme under the Marie Sklodowska-Curie grant agreement No. 778092 and from MINECO, project: MAT2017-83014-C2-1-P. The financial contribution of the Basque Government through grant IT1309-19 is gratefully acknowledged. We also thank ALBA Synchrotron facility for providing funding and beam time through the project: 2018072905 and the fellowship from the University of the Basque Country UPV/EHU.

ORCID IDs:

Idoia Arandia: 0000-0001-7097-719X

Leire Meabe: 0000-0003-1449-1544

Haritz Sardon: 0000-0002-6268-0916

David Mecerreyes: 0000-0002-0788-7156

Alejandro J. Müller: 0000-0001-7009-7715

3. REFERENCES

(1) Nair, L. S.; Laurencin, C. T. Biodegradable polymers as biomaterials. *Prog. Polym. Sci.* **2007,** *32*, 762-798.
(2) Rokicki, G., Aliphatic cyclic carbonates and spiroorthocarbonates as monomers. *Prog. Polym. Sci.* **2000**, *25*, 259-342.
(3) Siracusa, V.; Rocculi, P.; Romani, S.; Dalla Rosa, M. Biodegradable polymers for food packaging: a review. *Trends Food Sci. Tech.* **2008,** *19*, 634-643.
(4) Darensbourg, D. J.; Moncada, A. I. Tuning the Selectivity of the Oxetane and CO_2 Coupling Process Catalyzed by (Salen)CrCl/n-Bu_4NX: Cyclic Carbonate Formation vs Aliphatic Polycarbonate Production. *Macromolecules* **2010,** *43*, 5996-6003.
(5) Jaworska, J.; Kawalec, M.; Pastusiak, M.; Reczynska, K.; Janeczek, H.; Lewicka, K.; Pamula, E.; Dobrzynski, P. Biodegradable polycarbonates containing side carboxyl groups—synthesis, properties, and degradation study. *J. Polym. Sci., Part A: Polym. Chem.* **2017,** *55*, 2756-2769.
(6) Dai, Y.; Zhang, X. Cationic polycarbonates via ring-opening polymerization: design, synthesis, and applications. *Polym. Chem.* **2019,** *10*, 296-305.
(7) Chan, J. M. W.; Zhang, X.; Brennan, M. K.; Sardon, H.; Engler, A. C.; Fox, C. H.; Frank, C. W.; Waymouth, R. M.; Hedrick, J. L. Organocatalytic Ring-Opening Polymerization of Trimethylene Carbonate To Yield a Biodegradable Polycarbonate. *J. Chem. Educ.* **2015,** *92*, 708-713.
(8) Kamber, N. E.; Jeong, W.; Waymouth, R. M.; Pratt, R. C.; Lohmeijer, B. G. G.; Hedrick, J. L. Organocatalytic Ring-Opening Polymerization. *Chem. Rev.* **2007,** *107*, 5813-5840.
(9) Wang, C. F.; Lin, Y. X.; Jiang, T.; He, F.; Zhuo, R. X. Polyethylenimine-grafted polycarbonates as biodegradable polycations for gene delivery. *Biomaterials* **2009,** *30*, 4824-4832.
(10) Inoue, S.; Koinuma, H.; Tsuruta, T. Copolymerization of carbon dioxide and epoxide. *J. Polym. Sci., Part B: Polym. Lett.* **1969,** *7*, 287-292.
(11) Darensbourg, D. J. Copolymerization of Epoxides and CO_2: Polymer Chemistry for Incorporation in Undergraduate Inorganic Chemistry. *J. Chem. Educ.* **2017,** *94*, 1691-1695.
(12) Nakano, K.; Nakamura, M.; Nozaki, K. Alternating Copolymerization of Cyclohexene Oxide with Carbon Dioxide Catalyzed by (salalen)CrCl Complexes. *Macromolecules* **2009,** *42*, 6972-6980.
(13) Bossion, A.; Heifferon, K. V.; Meabe, L.; Zivic, N.; Taton, D.; Hedrick, J. L.; Long, T. E.; Sardon, H. Opportunities for organocatalysis in polymer synthesis via step-growth methods. *Prog. Polym. Sci.* **2019,** *90*, 164-210.
(14) Zhao, T. P.; Ren, X. K.; Zhu, W. X.; Liang, Y. R.; Li, C. C.; Men, Y. F.; Liu, C. Y.; Chen, E. Q. "Brill Transition" Shown by Green Material Poly(octamethylene carbonate). *ACS Macro Lett.* **2015,** *4*, 317-321.
(15) Zhu, W.; Zhou, W.; Li, C.; Xiao, Y.; Zhang, D.; Guan, G.; Wang, D. Synthesis, Characterization and Degradation of Novel Biodegradable Poly(butylene-co-hexamethylene carbonate) Copolycarbonates. *J. Macromol. Sci., A* **2011,** *48*, 583-594.
(16) Zhang, J.; Zhu, W.; Li, C.; Zhang, D.; Xiao, Y.; Guan, G.; Zheng, L. Effect of the biobased linear long-chain monomer on crystallization and biodegradation behaviors of poly(butylene carbonate)-based copolycarbonates. *RSC Adv.* **2015,** *5*, 2213-2222.
(17) Park, J. H.; Jeon, J. Y.; Lee, J. J.; Jang, Y.; Varghese, J. K.; Lee, B. Y. Preparation of High-Molecular-Weight Aliphatic Polycarbonates by Condensation Polymerization of Diols and Dimethyl Carbonate. *Macromolecules* **2013,** *46*, 3301-3308.
(18) Sun, J.; Kuckling, D. Synthesis of high-molecular-weight aliphatic polycarbonates by organo-catalysis. *Polym. Chem.* **2016,** *7*, 1642-1649.
(19) Nederberg, F.; Connor, E. F.; Möller, M.; Glauser, T.; Hedrick, J. L. New Paradigms for Organic Catalysts: The First Organocatalytic Living Polymerization. *Angew. Chem. Int. Ed.* **2001,** *40*, 2712-2715.

(20) Meabe, L.; Huynh, T. V.; Lago, N.; Sardon, H.; Li, C.; O'Dell, L. A.; Armand, M.; Forsyth, M.; Mecerreyes, D. Poly(ethylene oxide carbonates) solid polymer electrolytes for lithium batteries. *Electrochim. Acta* **2018,** *264*, 367-375.
(21) Meabe, L.; Lago, N.; Rubatat, L.; Li, C.; Müller, A. J.; Sardon, H.; Armand, M.; Mecerreyes, D. Polycondensation as a Versatile Synthetic Route to Aliphatic Polycarbonates for Solid Polymer Electrolytes. *Electrochim. Acta* **2017,** *237*, 259-266.
(22) Papageorgiou, G. Z.; Bikiaris, D. N. Synthesis and Properties of Novel Biodegradable/Biocompatible Poly[propylene-co-(ethylene succinate)] Random Copolyesters. *Macromol. Chem. Phys.* **2009,** *210*, 1408-1421.
(23) Pérez-Camargo, R. A.; Arandia, I.; Safari, M.; Cavallo, D.; Lotti, N.; Soccio, M.; Müller, A. J. Crystallization of isodimorphic aliphatic random copolyesters: Pseudo-eutectic behavior and double-crystalline materials. *Eur. Polym. J.* **2018,** *101*, 233-247.
(24) Fillon, B.; Wittmann, J. C.; Lotz, B.; Thierry, A. Self-nucleation and recrystallization of isotactic polypropylene (α phase) investigated by differential scanning calorimetry. *J. Polym. Sci., Part B: Polym. Phys.* **1993,** *31*, 1383-1393.
(25) Müller, A. J.; Arnal, M. L. Thermal fractionation of polymers. *Prog. Polym. Sci.* **2005,** *30*, 559-603.
(26) Lorenzo, A. T.; Arnal, M. L.; Sanchez, J. J.; Muller, A. J. Effect of annealing time on the self-nucleation behavior of semicrystalline polymers. *J. Polym. Sci., Part B: Polym. Phys.* **2006,** *44*, 1738-1750.
(27) Pan, P.; Inoue, Y. Polymorphism and isomorphism in biodegradable polyesters. *Prog. Polym. Sci.* **2009,** *34*, 605-640.
(28) Arandia, I.; Mugica, A.; Zubitur, M.; Arbe, A.; Liu, G.; Wang, D.; Mincheva, R.; Dubois, P.; Müller, A. J. How Composition Determines the Properties of Isodimorphic Poly(butylene succinate-ran-butylene azelate) Random Biobased Copolymers: From Single to Double Crystalline Random Copolymers. *Macromolecules* **2015,** *48*, 43-57.
(29) Tadokoro, H.; Chatani, Y.; Yoshihara, T.; Tahara, S.; Murahashi, S. Structural studies on polyethers, $[-(CH_2)m\text{-}O-]_n$. II. Molecular structure of polyethylene oxide. *Die Makromolekulare Chemie* **1964,** *73*, 109-127.
(30) Bunn, C. W. The crystal structure of long-chain normal paraffin hydrocarbons. The “shape” of the $<CH_2$ group. *Trans. Faraday Soc.* **1939,** *35*, 482-491.
(31) Pérez-Camargo, R. A.; Fernández-d’Arlas, B.; Cavallo, D.; Debuissy, T.; Pollet, E.; Avérous, L.; Müller, A. J. Tailoring the Structure, Morphology, and Crystallization of Isodimorphic Poly(butylene succinate-ran-butylene adipate) Random Copolymers by Changing Composition and Thermal History. *Macromolecules* **2017,** *50*, 597-608.
(32) Ciulik, C.; Safari, M.; Martínez de Ilarduya, A.; Morales-Huerta, J. C.; Iturrospe, A.; Arbe, A.; Müller, A. J.; Muñoz-Guerra, S. Poly(butylene succinate-ran-ε-caprolactone) copolyesters: Enzymatic synthesis and crystalline isodimorphic character. *Eur. Polym. J.* **2017,** *95*, 795-808.
(33) Mazzocchetti, L.; Scandola, M.; Jiang, Z. Random copolymerization with a large lactone enhances aliphatic polycarbonate crystallinity. *Eur. Polym. J.* **2012,** *48*, 1883–1891.
(34) Masubuchi, T.; Sakai, M.; Kojio, K.; Furukawa, M.; Aoyagi, T. Structure and Properties of Aliphatic Poly(carbonate) glycols with Different Methylene Unit Length. *E-J. Soft Mater.* **2007,** *3*, 55-63.
(35) Yu, Y.; Sang, L.; Wei, Z.; Leng, X.; Li, Y. Unique isodimorphism and isomorphism behaviors of even-odd poly(hexamethylene dicarboxylate) aliphatic copolyesters. *Polymer* **2017,** *115*, 106-117.
(36) Yu, Y.; Wei, Z.; Zhou, C.; Zheng, L.; Leng, X.; Li, Y. Miscibility and competition of cocrystallization behavior of poly(hexamethylene dicarboxylate)s aliphatic copolyesters: Effect of chain length of aliphatic diacids. *Eur. Polym. J.* **2017,** *92*, 71-85.
(37) Safari, M.; Martínez de Ilarduya, A.; Mugica, A.; Zubitur, M.; Muñoz-Guerra, S.; Müller, A. J. Tuning the Thermal Properties and Morphology of Isodimorphic Poly[(butylene succinate)-ran-

(ε-caprolactone)] Copolyesters by Changing Composition, Molecular Weight, and Thermal History. *Macromolecules* **2018,** *51*, 9589-9601.
(38) Papageorgiou, G. Z.; Bikiaris, D. N. Synthesis, cocrystallization, and enzymatic degradation of novel poly(butylene-co-propylene succinate) copolymers. *Biomacromolecules* **2007,** *8*, 2437-2449.
(39) Tan, B.; Bi, S.; Emery, K.; Sobkowicz, M. J. Bio-based poly(butylene succinate-co-hexamethylene succinate) copolyesters with tunable thermal and mechanical properties. *Eur. Polym. J.* **2017,** *86*, 162-172.